Journal of the Serbian Chemical Society
JSCS-info@shd.org.rs • www.shd.org.rs/JSCS
J. Serb. Chem. Soc. 80 (2) 237–251 (2015)
JSCS–4713
UDC 546.41'185+544.27+544.654.2:
621.793:539.217
Original scientific paper

The porosity and roughness of electrodeposited calcium phosphate coatings in simulated body fluid

MARIJA S. DJOŠIĆ[1], MIODRAG MITRIĆ[2] and VESNA B. MIŠKOVIĆ-STANKOVIĆ[3*#]

[1]Institute for Technology of Nuclear and Other Mineral Raw Materials, Franše d'Epere 86, 11000 Belgrade, Serbia, [2]Institute of Nuclear Sciences "Vinča", University of Belgrade, P. O. Box 522, 11001 Belgrade, Serbia and [3]Faculty of Technology and Metallurgy, University of Belgrade, Karnegijeva 4, P. O. Box 3503, 11120 Belgrade, Serbia

(Received 26 June, revised 1 October, accepted 2 October 2014)

Abstract: Calcium phosphate coatings were electrochemically deposited on titanium from an aqueous solution of $Ca(NO_3)_2$ and $NH_4H_2PO_4$ at a current density of 10 mA cm^{-2} for a deposition time of 15 min. The obtained brushite coatings ($CaHPO_4 \cdot 2H_2O$), were converted to hydroxyapatite (HA) by soaking in simulated body fluid (SBF) for 2, 7 and 14 days. The brushite and hydroxyapatite coatings were characterized by X-ray diffraction (XRD), scanning electron microscopy (SEM) and atomic force microscopy (AFM). It was shown that increasing the soaking time increased the porosity, roughness and crystallite domain size of the HA coatings and decreased the unit cell parameters and unit cell volume, while the mean pore area of HA was unaffected. The calcium and phosphorus ions concentrations in SBF were determined by atomic absorption spectroscopy (AAS) and UV–Vis spectroscopy, respectively, and a mechanism of HA growth based on dissolution–precipitation was proposed.

Keywords: hydroxyapatite; brushite; coatings; nanostructures; titanium.

INTRODUCTION

Metals have been used in various forms as implants due to their excellent mechanical properties, but lack of biocompatibility and corrosion resistance make metals inadequate for implantation in the body. The main reasons for applying ceramic coating on metal substrates are to protect the substrate against corrosion, to make the implant biocompatible and to turn the non-bioactive metal surface into a bioactive one.[1,2]

* Corresponding author. E-mail: vesna@tmf.bg.ac.rs
# Serbian Chemical Society member.
doi: 10.2298/JSC140626098D

The main constituents of human bone are calcium orthophosphates, collagen and water. Hydroxyapatite (HA, $Ca_{10}(PO_4)_6(OH)_2$), constitutes the majority of the inorganic component. HA is the only compound among calcium phosphate-based ceramics that is stable in a physiological environment and is biologically active. Applications of HA bioceramics are based on its excellent bioactivity, biocompatibility and porous structure. Both the micro- and macro-porosity of HA coatings are important. The macroporosity controls access of tissue and biological fluids to HA coatings. The microporosity controls protein adsorption, body fluid circulation and the resorption rate of calcium phosphate. The porous structure of HA improves the mechanical interlock between the cells and the surface of an implant, promotes osteoconductivity and enhances the adhesion between natural bone and an implant by the formation of an apatite layer.[3–5] Besides the coating porosity, a very important characteristic is the roughness of a coating, because the biocompatibility and corrosion resistance of implants are, also, determined by surface microstructural properties, such as surface roughness and grain size, which influence cell attachment, proliferation and differentiation.[6,7] There are a great number of methods for HA preparation,[8–12] including transformation of more soluble metastable phosphates, as precursors, *e.g.*, brushite, monetite and octacalcium phosphate, in an aqueous environment.[13–20]

The application of HA coatings depends on its crystallite size. It is possible to improve the characteristics of HA by controlling the particle size, particle distribution and agglomeration of precursors. Nanocrystalline HA exhibits a greater surface area and has better bioactivity than coarser crystals.[21–24]

Brushite, $CaHPO_4{\cdot}2H_2O$, is a metastable compound, known as mineral brushite. It can be observed when calcium phosphate is precipitated at low pH values and low temperatures.[20,25,26] As a precursor, brushite transforms into thermodynamically more stable calcium phosphates. Brushite can be converted to HA by alkaline treatment or by soaking in simulated body fluid (SBF).[20,27–31] The kinetics of brushite transformation to HA is of great importance because the success of osseointegration is defined by tissue–material integration during the early period of implantation.[32]

The aim of this work was to evaluate the ability of electrochemically deposited calcium phosphate coatings on titanium for conversion to HA in SBF solution. Additionally, the purpose was to investigate the influence of the soaking time in SBF on the composition and morphology (crystallite domain size, pore number, porosity, mean pore area and roughness) of the converted HA coatings. An attempt was made to propose a mechanism of HA growth on the electrodeposited calcium phosphate coatings on titanium.

EXPERIMENTAL

Electrochemical deposition of calcium phosphate coatings

Calcium phosphate coatings were electrochemically deposited on titanium plates (15 mm×10 mm×0.127 mm, Alfa Aesar, Johnson Matthew Co., purity: 99.7 %) from a stirred aqueous solution of 0.042 M $Ca(NO_3)_2$ and 0.025 M $NH_4H_2PO_4$. The initial pH value of the solution was 4.0. All chemicals were of reagent grade (Sigma–Aldrich) and used without further purification. The electrodeposition was performed at current density of 10 mA cm^{-2} for deposition time of 15 min.

Chronopotentiometric curve was recorded during the calcium phosphate deposition in a three-electrode cell arrangement using Gamry Reference 600 potentiostat–galvanostat/ZRA. The working electrode was titanium plate. The counter electrode was platinum plate, placed parallel to the working electrode. The saturated calomel electrode (SCE) was used as reference electrode. Prior to the deposition, titanium plates were degreased in acetone and then in ethanol for 15 min in an ultrasonic bath.

Conversion of the calcium phosphate coatings to hydroxyapatite upon soaking in SBF

The calcium phosphate coatings were soaked in SBF solution for 2, 7 and 14 days. SBF solution was prepared by dissolving the reagent-grade chemicals of NaCl, $NaHCO_3$, KCl, $K_2HPO_4{\cdot}3H_2O$, $MgCl_2{\cdot}6H_2O$, $CaCl_2$ and Na_2SO_4 in deionized water.[33] The prepared SBF solution was buffered with tris(hydroxymethyl)aminomethane, $(CH_2OH)_3CNH_2$, and the pH was fixed to 7.4 by the addition of 1.0 mol dm^{-3} HCl. For the experiments, the calcium phosphate coatings were placed in plastic containers and SBF was added. The containers were kept at a constant temperature of 37 °C. All the SBF solution was replaced by a fresh charge every 48 h.

X-Ray diffraction

The phase composition and structure of calcium phosphate coatings and HA coatings were determined by XRD, using a Philips PW 1050 diffractometer with CuK_α radiation (λ = 1.5418 Å) and Bragg–Brentano focusing geometry. Measurements were realized in the 2θ range of 8–70° with scanning step width of 0.05° and time of 6 s per point-step. The lattice parameters and crystallite domain size were obtained using the X-ray line profile-fitting program XFIT with a fundamental parameters convolution approach to generate line profiles.[34]

Atomic absorption spectroscopy

During soaking period of calcium phosphate coatings in SBF solution, the concentration of calcium ions was determined by atomic absorption spectroscopy, using a Perkin Elmer 703 atomic absorption spectrometer.

UV–Vis spectroscopy

During the soaking period, the concentration of phosphorus ions of the calcium phosphate coatings in the SBF solution was determined by UV–Vis spectroscopy, using a Philips UV–Vis 8610 spectrophotometer.

Scanning electron microscopy

The microstructure of calcium phosphate coatings and HA coatings was examined by SEM using a JSM-20 (JEOL) instrument. The micrographs were subjected to image analysis processing using Image-J software.[35] The images were converted to grayscale, thresholded to binary images and the pore area and porosity were estimated using Image-J software.

Atomic force microscopy

In order to characterize the surface topography of the calcium phosphate coatings and HA coatings, atomic force microscopy (AFM) was used. The measurements were performed using a Quesant Universal SPM instrument operating in the non-contact mode.

RESULTS AND DISCUSSION

Electrochemical deposition and characterization of calcium phosphate coatings on titanium

The chronopotentiometric curve for calcium phosphate electrodeposition in a solution containing 0.042 M $Ca(NO_3)_2$ and 0.025 M $NH_4H_2PO_4$, at a constant current density of 10 mA cm^{-2} for a deposition time of 15 min, is shown in Fig. 1.

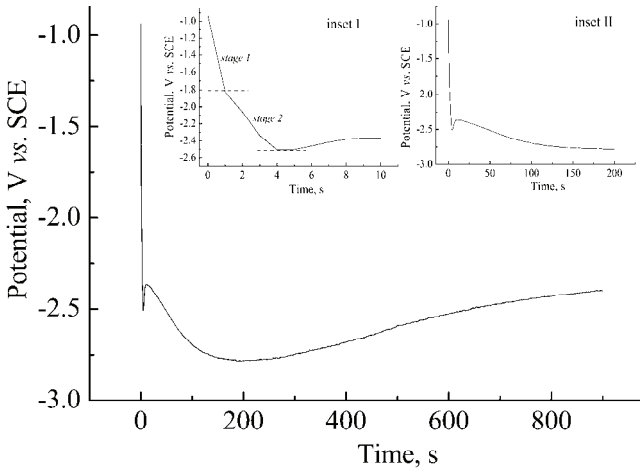

Fig. 1. Chronopotentiometric curve at a current density of 10 mA cm^{-2}.

For the initial very short time of deposition, up to 4 s, two stages could be distinguished (Fig. 1, inset I): stage 1, during the first second of deposition, with a corresponding potential of –1.8 V and stage 2, during the following 3 s of deposition, with a corresponding potential of about –2.5 V. The slopes of these two stages are different and suggest that stage 1 is a faster electrochemical reaction, and stage 2 is a slower reaction. This is in good agreement with proposed mechanism for electrochemical deposition of calcium phosphate coatings on titanium.[20,36,37] Briefly, at a potential up to –1.9 V, two processes occur: hydrogen reduction from NH_4^+ (originating from the starting $NH_4H_2PO_4$), which causes a local increase in pH (around 9) in the vicinity of the cathode and conversion of $H_2PO_4^-$, (originating from the starting $NH_4H_2PO_4$), into HPO_4^{2-}. In the presence of Ca^{2+} (originating from the starting $Ca(NO_3)_2$) and HPO_4^{2-}, brushite is deposited onto the cathode, which was confirmed by XRD analysis (Fig. 2):

$$Ca^{2+} + HPO_4^{2-} + 2H_2O \rightarrow CaHPO_4 \cdot 2H_2O \quad (1)$$

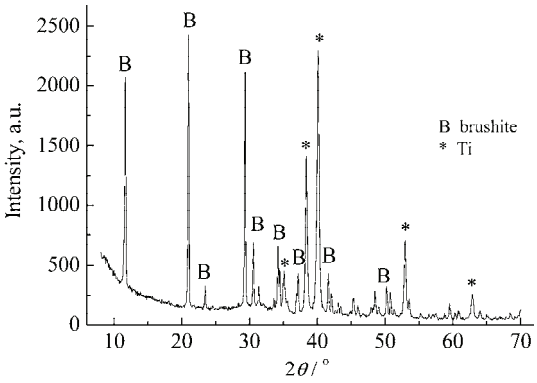

Fig. 2. XRD pattern of a brushite coating deposited on titanium.

Simultaneously, the brushite coating deposited at the cathode and hydrogen bubbles evolved on the cathode, causes a decrease in slope of chronopotentiometric curve (Fig. 1, inset I, stage 2). Namely, at potentials below –1.9 V, hydrogen evolution from water occurs, leading to the formation of a great number of H_2 molecules.[20] Hence, at the potentials up to –2.5 V, two parallel reactions occur: brushite deposition and growth and, on the other hand, the electrochemical reaction of hydrogen evolution. After the initial interval of 4 s, the electrochemical deposition of brushite occurs mainly through the porous film and this step is represented with maximum of the potential–time curve followed by decrease in the potential during further 200 s (Fig. 1, inset II). For deposition time longer than 200 s, the potential increases, suggesting that the H_2 bubbles are leaving the electrode surface.

The XRD pattern for the calcium phosphate coating electrochemically deposited on titanium is shown in Fig. 2. The identified diffraction maxima correspond to brushite, $CaHPO_4 \cdot 2H_2O$ (JCPDS No. 72-0713) and α-Ti as the substrate (JCPDS No. 89-3073).

SEM micrograph of the brushite coating is represented in Fig. 3, where the plate-like structure of the coating could be observed.

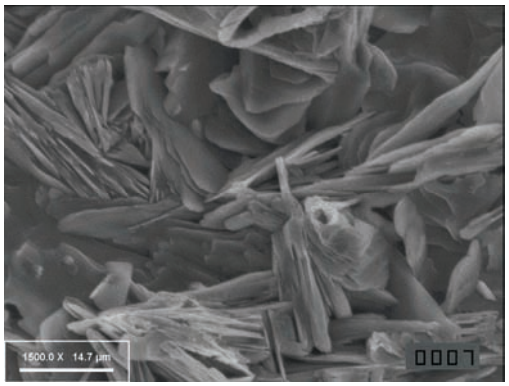

Fig. 3. SEM micrograph of a brushite coating.

The histogram of pore area distribution for a brushite coating, represented in Fig. 4, was determined using Image-J software. From Fig. 4, it could be seen that the majority of the pores had a pore area under 3 μm^2. The values of the mean pore area and percentage of surface covered by pores (porosity) were calculated to be 1.204 μm^2 and 4.88 %, respectively (Table I).

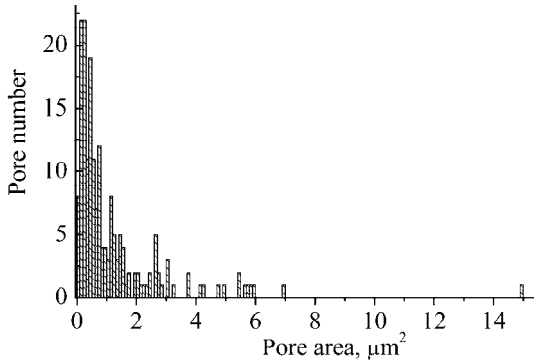

Fig. 4. Pore area distribution for a brushite coating.

TABLE I. Pore number, mean pore area, porosity and surface roughness of brushite and HA coatings after 7 and 14 days in SBF

Sample	Pore number	Mean pore area μm^2	Porosity %	Roughness	
				RMS / nm	R_a / nm
Brushite coating	186	1.204	4.88	148.4	125.7
HA coating (7 days in SBF)	329	0.492	6.30	294.8	231.1
HA coating (14 days in SBF)	510	0.475	9.41	726.4	567.0

The AFM surface topography of brushite coating is represented in Fig. 5 (10 × 10 μm area). The plate-like structure of the brushite coating could be observed, while the roughness parameters, RMS and R_a, amount to 148.4 and 125.7 nm, respectively (Table I).

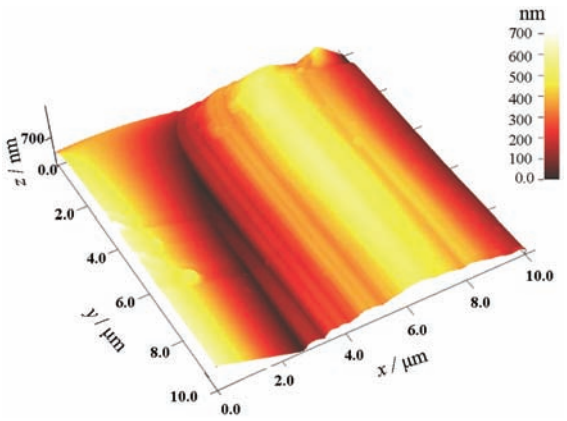

Fig. 5. AFM micrograph of a brushite coating.

Hydroxyapatite coatings on titanium

XRD analysis. The XRD patterns of the converted coatings, obtained after soaking the brushite coating in SBF for 2, 7 and 14 days, are represented in Fig. 6. The phase composition of converted coatings corresponded to hydroxyapatite, $Ca_{10}(PO_4)_6(OH)_2$ (JCPDS No. 86-1199) and α-Ti (originating from the substrate). The absence of diffraction maximums for brushite confirmed that the complete surface, primarily coated with brushite, was fully converted to HA.

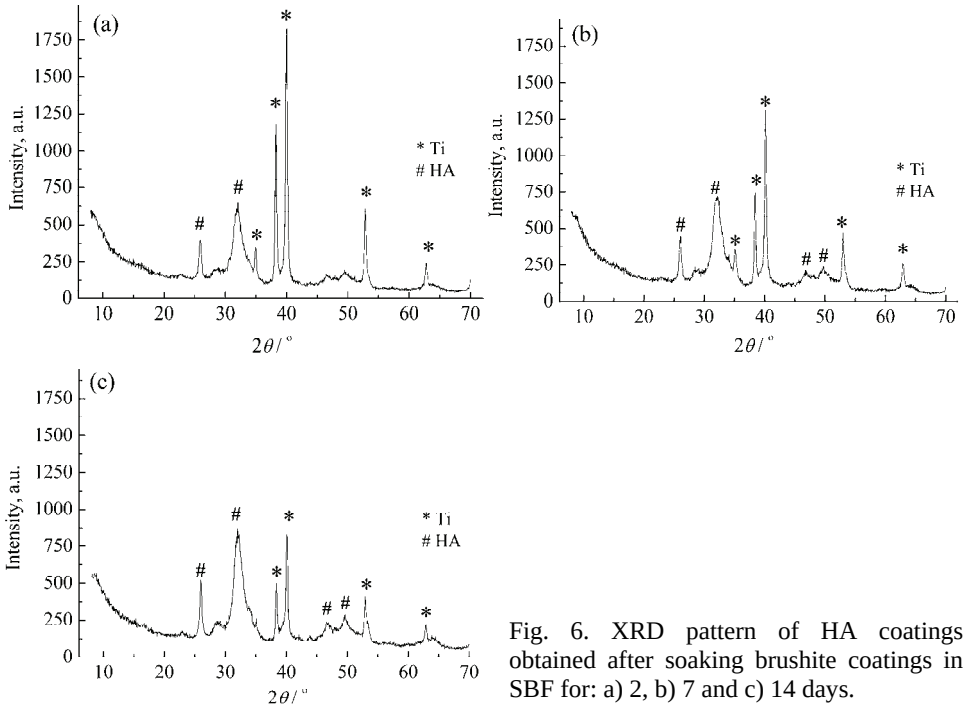

Fig. 6. XRD pattern of HA coatings obtained after soaking brushite coatings in SBF for: a) 2, b) 7 and c) 14 days.

The crystallite domain size, calculated for the (002) plane, as well as the unit cell parameters and unit cell volume for the HA coatings obtained after soaking the brushite coatings in SBF for 2, 7 and 14 days, are presented in Table II.

TABLE II. The crystallite domain size, unit cell parameters, *a* and *c*, and unit cell volume, *V*, for HA coatings obtained after soaking of brushite coatings for 2, 7 and 14 days in SBF

Days in SBF	Crystallite domain size, nm	Unit cell parameters, Å		Unit cell volume, Å^3
		a	*c*	
2	14.4	9.5111	6.9585	545.14
7	15.0	9.5105	6.9487	544.30
14	16.2	9.4843	6.9265	539.58

The results suggest that increasing the soaking time slightly increased the crystallite domain size of the converted HA coatings and decreased the unit cell parameters and unit cell volume, because of the increased crystal density.

In vitro *tests of HA coating in SBF*

In order to investigate the mechanism of brushite conversion to HA, the concentrations of Ca and P ions during 14 days of immersion of the brushite coating in SBF solution were determined by AAS and UV–Vis spectroscopy, respectively. The dependences of the concentrations of Ca and P ions in SBF on the soaking time are presented in Fig. 7a and b, respectively. For shorter immersion times, during the first two days, rapid decreases in both the concentrations of Ca and P ions were observed. Namely, the high rate of consumption of Ca and P ions indicates the high reactivity of brushite with SBF that induces the transformation of brushite and the nucleation of HA. XRD results for the HA coating observed after two days of immersion (Fig. 6a), confirmed that the brushite had completely transformed to HA, indicating the ability of brushite to generate HA by intake of Ca and P ions from the surrounding solution. This is in good agreement with the literature.[33,38] Namely, once immersed in SBF (pH 7.4), brushite dissolves rapidly because brushite is stable under acidic aqueous conditions at pH < 4.2. The increase in the local concentration of Ca and P ions resulted in the precipitation of calcium phosphates. Bearing in mind that the pH of the SBF was 7.4 and that SBF is supersaturated with respect to apatite (the Ca/P mole ratio was 2.50), the only stable phase that could be precipitated is HA. The rapid formation of a Ca and P rich layer in a relatively short time of immersion is of special interest because the success of osseointegration is defined by tissue–material interaction during the early days of implantation.[32,39,40]

In general, both dissolution and precipitation of calcium phosphates occur simultaneously, but the kinetics of these two processes are different. The dissol-

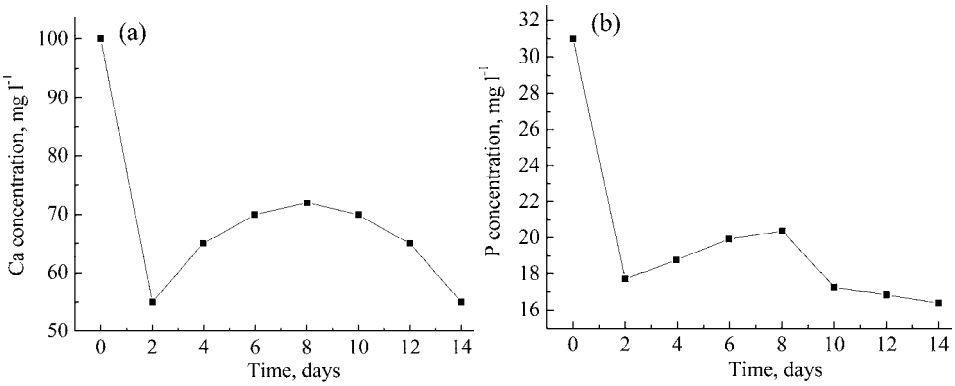

Fig. 7. The dependences of (a) the Ca concentration and (b) the P concentration in SBF on the soaking time of brushite coating.

ution process is governed by ion exchange, while the precipitation process is controlled by the product of the ion concentrations and the solubility of the particles. The dissolution and precipitation of calcium phosphates in SBF is a reversible reaction.[41–43]

The increase in the Ca concentration between days 2 and 8 of immersion is shown in Fig. 7a, meaning that the precipitation rate decreased, while the dissolution rate increased. After 8 days of immersion, the concentration of Ca ions decreased, indicating that further precipitation of HA coating dominated over dissolution. Indeed, the increase in the mass of the HA coating during exposure to SBF solution (6.6, 13.8 and 19.0 mg after 2, 7 and 14 days, respectively) confirmed that precipitation of HA coating prevailed.

The increase in the P ions concentration between day 2 and 8 of immersion is shown in Fig. 7b, suggesting that the precipitation rate slowed down, while the dissolution rate increased. The HA coating dissolution created a great number of the nucleation sites on the coating surface. During longer immersion time (between 8 to 14 days), a decrease in P ions concentration could be observed, indicating the consumption of P ions during soaking.

SEM analysis of HA coatings

The SEM micrographs of the HA coatings after soaking in SBF for 7 and 14 days are presented in Figs. 8a and 9a, respectively. Figure 8a shows the agglomerated sphere-like crystallites of different size after 7 days of immersion, while after 14 days (Fig. 9a), the morphology of the coating had changed and less agglomerates could be observed. The SEM micrographs of HA coatings were analyzed by "Image-J" software.[35] After 7 days of soaking, the surface of the HA coating was fully covered by a HA layer, which was confirmed by XRD (Fig. 6b). A 3D plot of a sphere-like agglomerate, with a size of approximately 4.0 μm in diameter is presented in Fig. 8b (detail from Fig. 8a, marked with an arrow). The sphere-like agglomerate consisted of very fine crystallites, suggesting a high

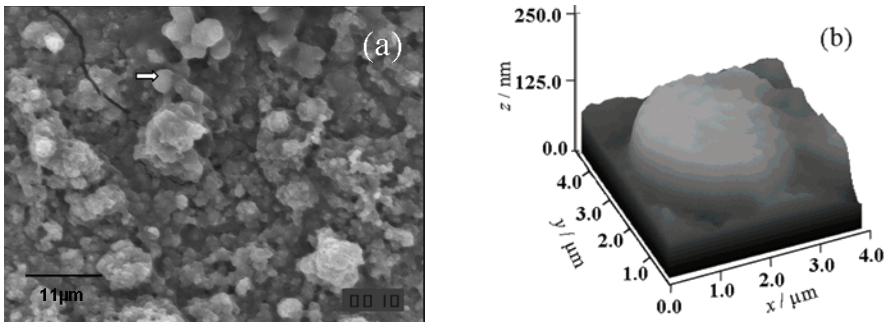

Fig. 8. SEM micrograph of: a) an HA coating obtained by soaking a brushite coating in SBF for 7 days and b) a 3D plot of the sphere-like agglomerate marked with an arrow in (a).

nucleation rate of HA. After a soaking period of 14 days, the HA coating surface had fewer agglomerates. A new spherical particle, with a size of approximately 1.0 μm in diameter, presented in Fig. 9b (the detail from Fig. 9a, marked with arrow), appeared on the surface of the previously precipitated HA as a consequence of further deposition of HA with soaking time.[44] Namely, when calcium phosphates were incubated in SBF solution, the formation of HA layer on the surface of the coating occurs, including dissolution, precipitation and growth of HA.[4,45,46] The formation of new agglomerates of HA on the surface of the previously precipitated hydroxyapatite, observed on the SEM micrographs (Fig. 9b), is in good agreement with results presented in Fig. 7, where the decrease in the concentration of Ca and P ions, after 8 days of soaking can be attributed to further HA precipitation. The formation of HA is very important in the formation of chemical bonds between tissue and bioactive material.

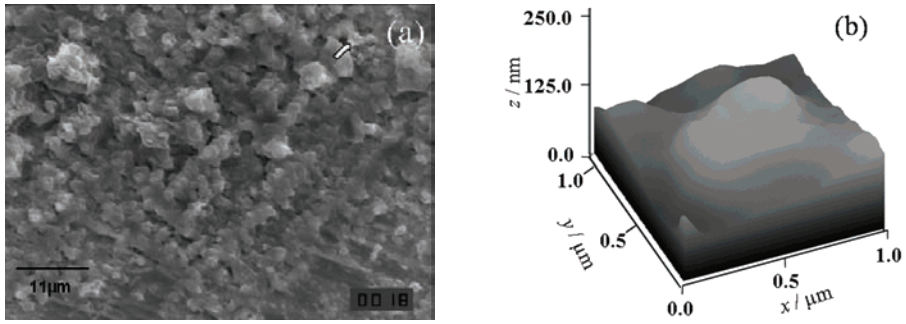

Fig. 9. SEM micrograph of: a) an HA coating obtained by soaking a brushite coating in SBF for 14 days and b) a 3D plot of the sphere-like agglomerate marked with an arrow in (a).

The pore area distribution for HA coatings, obtained after soaking in SBF for 7 and 14 days, using Image-J software, are represented in Fig. 10a and b, respectively.

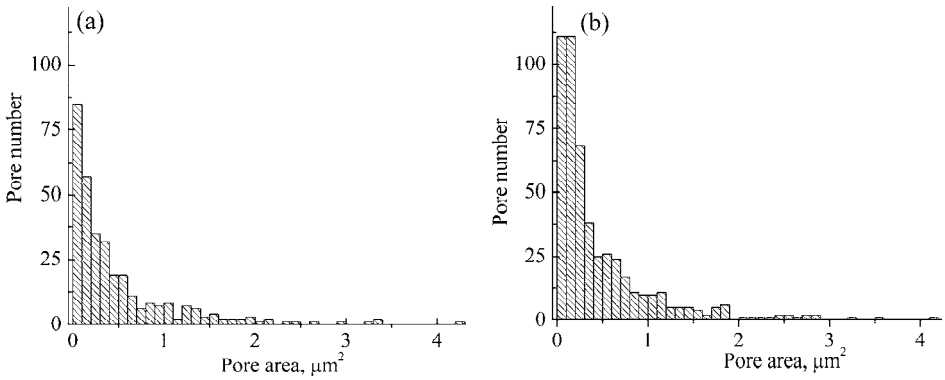

Fig. 10. Pore area distribution for HA coatings obtained by soaking brushite coatings in SBF for: a) 7 and b) 14 days.

The values of the number of pores, mean pore area and porosity, and the roughness parameters of the brushite and HA coatings obtained after soaking in SBF for 7 and 14 days are presented in Table I.

The brushite coating exhibited a relatively small number of pores (Table I) with a larger pore area. Upon soaking the brushite coating in SBF, since the conversion process occurred, the pore number increased significantly, while the mean pore area decreased during soaking for 14 days. Comparison of the histograms of the pore area distribution for HA coatings upon soaking for 7 and 14 days (Fig. 10a and b, respectively), indicates that the majority of the pores had a small pore area, up to 1 μm^2, and that there were only a small number of pores having a larger area. In addition, increasing the soaking time from 7 to 14 days increased the number of pores with areas up to 1 μm^2. Consequentially, the porosity of the HA coating increased with increasing soaking time, while the mean pore area did not change significantly. The increase in porosity of the HA coating for longer soaking times could be attributed to the simultaneous dissolution and precipitation of HA under physiological conditions, whereby precipitation dominates, which was confirmed by the increase in the mass of the HA coating, as was discussed earlier. Microporosity is very important parameter because it influences the adsorption of proteins by providing a greater surface area, as well as bone-like apatite formation by dissolution and precipitation.[47] Thus, it could be proposed that the HA coatings obtained after 14 days of soaking might have better protein adsorption ability due to their greater porosity with respect to HA coatings obtained after 7 days of soaking in SBF.

AFM analysis of HA coatings

AFM analysis of HA coatings obtained after soaking of brushite coatings in SBF for 7 and 14 days are represented in Fig. 11.

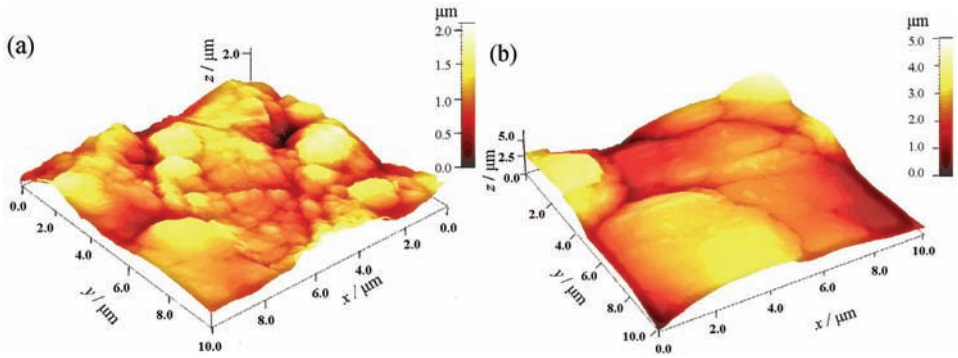

Fig. 11. AFM micrographs of HA coatings obtained by soaking brushite coatings in SBF for: a) 7 and b) 14 days.

Roughness is represented by the arithmetical mean deviation, R_a, and root mean square deviation, RMS. The results of the statistical analysis of the AFM micrographs for both the brushite and HA coatings are listed in Table I. The RMS and R_a values of the brushite coating were smaller than the corresponding values for the HA coating. Moreover, the RMS and R_a values of HA coatings increase with increasing soaking time from 294.8 nm to 726.4 nm and from 231.1 to 567.0 nm, respectively. According to the literature, an increase in the surface roughness of HA surfaces increases osteoblastic cell adhesion, proliferation and detachment strength.[6,48,49] On the other hand, a problem with highly rough surfaces is connected with cellular mobility. It was reported[7] that osteoclastogenesis could be induced if surface roughness, R_a, achieves values between 0.04 and 0.58 μm. This means that the present results are comparable with the results from the literature. The HA coatings obtained in SBF from brushite coating electrochemically deposited on titanium at constant current density could stimulate a cellular response.

CONCLUSIONS

In order to investigate the ability of HA formation on titanium substrate from brushite precursor under *in vitro* conditions, electrochemical deposition of a brushite coatings on titanium was performed galvanostatically at a current density of 10 mA cm^{-2} for a deposition time of 15 min.

The brushite coatings were soaked in an SBF solution and conversion to HA coatings was monitored by XRD, SEM, AFM, AAS and UV–Vis spectroscopy during *in vitro* tests. Increase in soaking time slightly increases the crystallite domain size of the HA coatings and decreases the unit cell parameters and unit cell volume, because of increased crystal density. Moreover, an increase in soaking time increased the mass, roughness, pore number and porosity of the HA coating, whereas the mean pore area was not significantly affected.

An *in vitro* study was used to investigate the biological response of HA coatings under physiological conditions and Ca and P ions concentration in SBF were determined, confirming the dissolution–precipitation mechanism. Since the crystallite domain size slightly increased, it could be proposed that nucleation of HA dominates over crystal growth and, consequently, an increase in coating roughness was observed, suggesting that precipitation of HA occurred through heterogeneous nucleation. Bearing in mind that increasing the soaking time increased the mass of the HA coating, it could be proposed that precipitation dominate over dissolution.

Based on all experimental results, it could be concluded that the increase in the HA coating porosity and coating roughness, resulting in a larger surface area, make this coating suitable for biomedical applications, because it is believed that the porosity contributes to better protein adsorption as well as bone-like apatite formation by the dissolution and precipitation mechanism. Additionally, the inc-

rease in HA coatings roughness indicates that the HA coatings could stimulate cellular response.

Acknowledgements. This research was financed by the Ministry of Education, Science and Technological Development, Republic of Serbia, contracts Nos. III 45019, III 45015 and OI 172004. The authors would like to thank Dr. Zoran Stojanović, Vinča Institute of Nuclear Sciences, University of Belgrade, for his help in the AFM measurements.

И З В О Д

ПОРОЗНОСТ И ХРАПАВОСТ ЕЛЕКТРОХЕМИЈСКИ ТАЛОЖЕНИХ ПРЕВЛАКА КАЛЦИЈУМ-ФОСФАТА У СИМУЛИРАНОЈ ТЕЛЕСНОЈ ТЕЧНОСТИ

МАРИЈА С. ЂОШИЋ[1], МИОДРАГ МИТРИЋ[2] и ВЕСНА Б. МИШКОВИЋ-СТАНКОВИЋ[3]

[1]Институт за технологију нуклеарних и других минералних сировина, Франше д'Епереа 86, 11000 Београд [2]Институт за нуклеарне науке "Винча", Универзитет у Београду, 11001 Београд и [3]Технолошко–металуршки факултет, Универзитет у Београду, Карнегијева 4, 11120 Београд

Превлаке калцијум-фосфата су електрохемијски таложене на титану из воденог раствора $Ca(NO_3)_2$ и $NH_4H_2PO_4$ при густини струје од 10 mA cm^{-2} за време од 15 мин. Добијене превлаке брушита ($CaHPO_4{\cdot}2H_2O$) су конвертоване у хидроксиапатит у симулираној телесној течности током 2, 7 и 14 дана. Превлаке брушита и хидроксиапатита су карактерисане дифракцијом X-зрака, скенирајућом електронском микроскопијом и микроскопијом атомских сила. Показано је да са продужавањем времена конверзије у симулираној телесној течности долази до повећања порозности, храпавости и величине кристалита превлаке хидроксиапатита, али и смањења параметара јединичне ћелије и запремине јединичне ћелије хидроксиапатита. Са друге стране, време конверзије не утиче на средњу површину пора превлака хидроксиапатита. Концентрације јона калцијума и фосфора у симулираној телесној течности одређиване су атомском апсорпционом спектроскопијом и UV–Vis спектроскопијом, редом. Предложен је механизам раста хидроксиапатита у симулираној телесној течности, базиран на теорији растварање–таложење.

(Примљено 26. јуна, ревидирано 1. октобра, прихваћено 2. октобра 2014)

REFERENCES

1. C. B. Carter, M. G. Norton, *Ceramic Materials Science and Engineering*, Springer, New York, 2007, p. 645
2. A. Janković, S. Eraković, A. Dindune, Dj. Veljović, T. Stevanović, Dj. Janaćković, V. Mišković-Stanković, *J. Serb. Chem. Soc.* **77** (2012) 1
3. F. Zeng, J. Wang, Y. Wu, Y. Yu, W. Tang, M. Yin, C. Liu, *Colloids Surfaces, A* **441** (2014) 737
4. P. N. Chavan, M. M. Bahir, R. U. Mene, M. P. Mahabole, R. S. Khairnar, *Mater. Sci. Eng., B* **168** (2010) 224
5. Dj. Veljović, R. Jančić-Hajneman, I. Balać, B. Jokić, S. Putić, R. Petrović, Dj. Janaćković, *Ceram. Int.* **37** (2011) 471
6. B. D. Hahn, D. S. Park, J. J. Choi, J. Ryu, W. H. Yoon, J. H. Choi, J. W. Kim, Y. L. Cho, C. Park, H. E. Kim, S. G. Kim, *Appl. Surf. Sci.* **257** (2011) 7792
7. J. Costa-Rodrigues, A. Fernandes, M. A. Lopes, M. H. Fernandes, *Acta Biomater*. **8** (2012) 1137
8. M. P. Ferraz, F. J. Monteiro, C. M. Manuel, *J. Appl. Biomater. Biom.* **2** (2004) 74

9. M. S. Djošić, V. B. Mišković-Stanković, S. Milonjić, Z. M. Kačarević-Popović, N. Bibić, J. Stojanović, *Mater. Chem. Phys.* **111 (**2008) 137
10. B. Bracci, S. Panzavolta, A. Bigi, *Surf. Coat. Technol.* **232** (2013) 13
11. S. Eraković, Dj. Veljović, P. N. Diouf, T. Stevanović, M. Mitrić, Dj. Janaćković, I. Z. Matić, Z. D. Juranić, V. Mišković-Stanković, *Prog. Org. Coat.* **75** (2012) 275
12. S. Eraković, Dj. Veljović, P. N. Diouf, T. Stevanović, M. Mitrić, S. Milonjić, V. B. Mišković-Stanković, *Int. J. Chem. React. Eng.* **7** (2009) A62
13. R. Štulajterová, L'. Medvecký, *Colloids Surfaces, A* **316** (2008) 104
14. W. Jiang, X. Chu, B. Wang, H. Pan, X. Xu, R. Tang, *J. Phys. Chem., B* **113** (2009) 10838
15. J. A. Juhasz, S. M. Best, A. D. Auffret, W. Bonfield, *J. Mater. Sci: Mater. Med.* **19** (2008) 1823
16. R. Horváthová, L. Müller, A. Helebrant, P. Greil, F. A. Müller, *Mater. Sci. Eng., C* **28** (2008) 1414
17. J. Hu, C. Wang, W. C. Ren, S. Zhang, F. Liu, *Mater. Chem. Phys.* **119** (2010) 294
18. A. V. Zavgorodniy, O. Borrero-López, M. Hoffman, R. Z. LeGeros, R. Rohanizadeh, *J. Mater. Sci: Mater. Med.* **22** (2011) 1
19. M. S. Djosic, V. B. Miskovic-Stankovic, Z. M. Kacarevic-Popovic, B. M. Jokic, N. M. Bibic, M. N. Mitric, S. K. Milonjic, R. M. Jancic-Heinemann, J. N. Stojanovic, *Colloids Surfaces, A* **341** (2009) 110
20. M. S. Djošić, V. Panić, J. Stojanović, M. Mitrić, V. B. Mišković-Stanković, *Colloids Surfaces, A* **400** (2012) 36
21. L. M. Rodríguez-Lorenzo, M. Vallet-Regí, *Chem. Mater.* **12** (2000) 2460
22. M. H. Fathi, V. Mortazavi, S. I. R. Esfahani, *Dent. Res. J.* **5** (2008) 81
23. R. Murugan, S. Ramakrishna, *J. Cryst. Growth* **274** (2005) 209
24. A. Hanifi, M. H. Fathi, *Iranian J. Pharm Sci.* **4** (2008) 141
25. H. E. L. Madsen, G. Thorvardarson, *J. Cryst. Growth* **66** (1984) 369
26. A. C. Tas, S. B. Bhaduri, *Ceram. Trans.* **164** (2005) 119
27. W. J. Shih, Y. H. Chen, S. H. Wang, W. L. Li, M. H. Hon, M. C. Wang, *J. Cryst. Growth* **285** (2005) 633
28. A. C. Tas, S. B. Bhaduri, *J. Am. Ceram. Soc.* **87** (2004) 2195
29. J. Peña, I. Izquierdo-Barba, A. Martínez, M. Vallet-Regí, *Solid State Sci.* **8** (2006) 513
30. J. H. Park, D. Y. Lee, K. T. Oh, Y. K. Lee, K. N. Kim, *J. Am. Ceram. Soc.* **87** (2004) 1792
31. A. Rakngarm, Y. Mutoh, *Mater. Sci. Eng., C* **29** (2009) 275
32. M. L. R. Schwarz, M. Kowarsch, S. Rose, K. Becker, T. Lenz, L. Jani, *J. Biomed. Mater. Res., A* **89** (2009) 667
33. T. Kokubo, H. Takadama, *Biomaterials* **27** (2006) 2907
34. R. W. Cheary, A. A. Coelho, *J Appl. Cryst.* **25** (1992) 109
35. ImageJ-Image processing and analysis in Java. Available on Web site: http:// //rsb.info.nih.gov/ij on 21.2.2015
36. N. Dumelié, H. Benhayoune, C. Rousse-Bertrand, S. Bouthors, A. Perchet, L. Wortham, J. Douglade, D. Laurent-Maquin, G. Balossier, *Thin Solid Films* **492** (2005) 131
37. E. A. Abdel-Aal, D. Dietrich, S. Steinhaeuser, B. Wielage, *Surf. Coat. Technol.* **202** (2008) 5895
38. M. C. Kuo, S. K. Yen, *J. Mater. Sci.* **39** (2004) 2357
39. M. Bohner, J. Lemaitre, *Biomaterials* **30** (2009) 2175
40. X. Lu, Y. Leng, *Biomaterials* **26** (2005) 1097
41. Q. Zhang, J. Chen, J. Feng, Y. Cao, C. Deng, X. Zhang, *Biomaterials* **24** (2003) 4741

42. M. Kumar, H. Dasarathy, C. Riley, *J. Biomed. Mater. Res.* **45** (1999) 302
43. R. Sun, K. Chen, Y. Lu, *Mater. Res. Bull.* **44** (2009) 1939
44. J. X. Zhang, R. F. Guan, X. P. Zhang, *J. Alloys Compd.* **509** (2011) 4643
45. H. Kim, R. P. Camata, S. Chowdhury, Y. K. Vohra, *Acta Biomater.* **6** (2010) 3234
46. S. Eraković, A. Janković, Dj. Veljović, E. Palcevskis, M. Mitrić, T. Stevanović, Dj. Janaćković, V. Mišković-Stanković, *J. Phys. Chem., B* **117** (2013) 1633
47. K. A. Hing, *Int. J. Appl. Ceram. Technol.* **2** (2005) 184
48. D. D. Deligianni, N. D. Katsala, P. G. Koutsoukos, Y. F. Missirlis, *Biomaterials* **22** (2001) 87
49. S. Sandukas, A. Yamamoto, A. Rabiei, *J. Biomed. Mater. Res., A* **97** (2011) 490.